Quantum-well theory of the exchange coupling in magnetic multilayers with application to Co/Cu/Co(001)

J. Mathon, Murielle Villeret, and A. Umerski
Department of Mathematics, City University, London EC1V 0HB, United Kingdom

R. B. Muniz and J. d'Albuquerque e Castro
Departamento de Fisica, Universidade Federal Fluminense, Niteroi, Brazil

D. M. Edwards
Department of Mathematics, Imperial College, London SW7 2BZ, United Kingdom
(Received 27 September 1996; revised manuscript received 14 March 1997)

Two parallel calculations of the exchange coupling in a Co/Cu/Co(001) trilayer, both using the same realistic s, p, and d tight-binding bands with parameters determined from the *ab initio* band structures of bulk Cu and Co, are reported. The coupling is first calculated within the framework of the quantum-well (QW) formalism in which the periodic behavior of the spectral density is exploited to derive an analytic formula for the coupling valid for large spacer thicknesses. On the other hand, an alternative expression for the coupling, referred to as cleavage formula, is derived that allows accurate and efficient numerical evaluation of the coupling. An analytic approximation to this expression, valid in the asymptotic region of large spacer thickness, is also obtained. These two approaches are discussed in relation to other existing theoretical formulations of the coupling. The numerical results for the coupling obtained from the cleavage formula are first compared with the analytical QW calculation. The agreement between the two calculations is impressive and entirely justifies the analytical QW approach. The numerical calculation fully confirms the result of the QW formalism that, for trilayers with thick Co layers, the short-period oscillation due to the minority electrons from the vicinity of the Cu Fermi-surface (FS) necks is dominant, the contribution of the long-period oscillation being negligible. This is shown, in the analytical QW formalism, to be due to the existence of bound states for the minority-spin electrons at the Cu FS necks in the ferromagnetic configuration. The dominant short-period oscillation has been confirmed by spin-polarized scanning electron microscopy and observed directly in the most recent photoemission experiments. The full confinement of the minority electrons at the neck of the Cu FS also leads to a strong temperature dependence of the short-period oscillation and an initial decay of the coupling with spacer thickness N that is much slower than predicted by the usual $1/N^2$ law. For the electrons at the belly of the Cu FS, the confinement is weak in both spin channels and the long-period oscillation hardly changes between zero and room temperatures. In addition, the belly contribution to the coupling decreases at $T=0$ K following the usual $1/N^2$ dependence. The amplitude of the calculated coupling ≈ 1.2 mJ/m^2 at the first antiferromagnetic peak of Cu is only a factor of 3 larger than the observed coupling strength. Finally, the coupling for 2 ML of Co embedded in Cu has also been evaluated from the cleavage formula. A large initial coupling strength (3.4 mJ/m^2) and comparable contributions from the short- and long-oscillation periods are obtained. This is in complete agreement with theoretical results reported by other groups. [S0163-1829(97)04138-6]

I. INTRODUCTION

Since the discovery of oscillatory exchange coupling[1] and the related giant magnetoresistance effect,[2] metallic magnetic multilayers have been studied extensively (for a review, see Ref. 3). In particular, a large number of theoretical approaches have been developed to calculate the oscillatory exchange coupling. They can be broadly divided into two categories: numerical total-energy calculations and calculations based on analytical asymptotic expansions. In the past, these two types of theory have coexisted but no meaningful quantitative comparison between them was possible because the analytical theories were originally developed only for simplified model band structures. This situation is highly unsatisfactory since our physical understanding of the oscillatory exchange coupling is based entirely on the theories of the latter type, in particular, on the quantum-well theory proposed by Edwards and Mathon[4] (see also Refs. 5–7). An alternative interpretation of the quantum-well theory in terms of reflection coefficients at the interfaces[8,9] is also widely used. There is now no doubt about the validity of the quantum-well picture since the quantum-well states predicted in Ref. 4 have been observed in photoemission experiments.[10–12] However, to achieve a unification between the analytical and numerical approaches, the quantum-well theory needs to be implemented for a fully realistic band structure and shown to be as accurate (in the asymptotic limit of a thick spacer) as fully numerical calculations.

In this paper, we report the results of two parallel calculations of the exchange coupling in a Co/Cu/Co(001) trilayer. One is based on the analytical quantum-well theory,[4–7] and the other is fully numerical. Both calculations were made using the same realistic s,p,d tight-binding bands fitted to *ab initio* band structures of bulk Cu and ferromagnetic fcc Co,

which means that they are directly comparable. The results of such a comparison were briefly reported in Ref. 13. The main motivation for writing a long paper is to provide a comprehensive description of both our calculations and to set clearly the analytical quantum-well theory in the context of the *ab initio* calculations. We shall also present additional numerical results for a Co/Cu/Co(001) trilayer based on a method for calculating the local one-electron Green's functions[15] that enables us to determine the coupling for continuous spacer layer thicknesses.

Since the precise relationship between the quantum-well theory based on the stationary-phase approximation (SPA) method and the *ab initio* calculations has been matter of some controversy, we first address this issue. In the first-principles spin-density-functional calculations, the self-consistency in each atomic plane is achieved separately in the ferromagnetic (FM) and antiferromagnetic (AF) configurations of the magnetic layers (see, e.g., Refs. 16 and 17 and some of the calculations in Ref. 18). However, such calculations are only feasible for relatively thin spacer layers of some 20–30 atomic planes and this is often not enough for the periods, amplitudes and phases of the coupling to be determined reliably. The Co/Cu/Co(001) trilayer is a prime example. It is apparent already from the numerical results of Drchal *et al.*[19] that one needs to go to a very large number of atomic planes of Cu to obtain reliable fits for this system. We show that this problem arises because the expected asymptotic decay of the coupling, assumed in all numerical fits, is not obeyed in Co/Cu at zero temperature even for Cu thicknesses as large as 50 atomic planes. We also show that, at room temperature (relevant to experiment), there is no range of Cu thicknesses in which the coupling amplitude can be approximated by a dependence $\propto 1/N^2$.

Because of these problems, the approach almost universally adopted now[19–22] is to use atomic potentials that are independent of the magnetic configuration and to calculate the total-energy difference by comparing sums of one-electron energies, thus making the approximation known as the ''force theorem.'' Once this approximation is made, the SPA method is applicable and must reproduce correctly the results of all such calculations in the limit of a thick spacer. This is because the SPA method provides merely a prescription for evaluating the energy and k-space sums of the one-electron energies analytically. It will be shown in Sec. II that the implementation of the SPA theory relies only on the fact that the one-electron Green's function is a periodic or quasi-periodic function of the spacer thickness.[14,15,23] This feature is common to the tight-binding method we use, linear-muffin-tin-orbital (LMTO) tight binding,[22] and layer Korringa-Kohn-Rostoker methods,[20] since they are all formulated in terms of local one-electron Green's functions. It is, therefore, immaterial which one of these methods one chooses as long as the one-electron energies of the multilayer are correctly reproduced.

The only remaining issue is the question of a correct treatment of interfaces. Far from the interface, one can, of course, use the potentials for bulk metals. Near the interface, the potentials may deviate from their bulk values. However, it is clear from the above discussion that this effect can be included in the SPA method based on our empirical tight-binding approach but a preliminary *ab initio* calculation in the interfacial region would be required to determine the correct local tight-binding on-site potentials and hopping parameters. Alternatively (and preferably), the SPA could be applied directly to, say, the LMTO tight-binding method with self-consistent treatment of the interface included. However, in the case of Co/Cu considered here, the LMTO calculations for a Co/Cu interface[24] show that it is an excellent approximation to use bulk Co and Cu potentials right up to the interface and this is, indeed, the approximation that is made in the calculations of the coupling for Co/Cu based on this method.[19,22] We have, therefore, adopted the same approximation here.

The plan of the paper is as follows. In Sec. II we show how the quantum-well SPA calculation is implemented for a Co/Cu/Co(001) trilayer using realistic s, p, and d tight-binding bands fitted to an *ab initio* band structure of bulk Cu and ferromagnetic fcc Co. In this calculation, the SPA method is applied directly to the spectral density that determines the thermodynamic potential of the trilayer.

For the numerical calculation, we use an expression for the coupling referred to as a cleavage formula. Its derivation is presented in Sec. III. The cleavage formula is obtained by introducing the Green's-function cleavage plane formalism[25] of the spin-current (torque) approach[26] in the formulation of d'Albuquerque e Castro, Ferreira, and Muniz.[27] The resultant cleavage formula for the coupling is equivalent to that developed independently by Drchal *et al.*[19] in their LMTO approach and has already been used without derivation in Refs. 13,14, and 28.

The cleavage formula is evaluated using a new analytic expression for slab one-electron Green's functions derived recently by Umerski.[15] The results of this fully numerical calculations are described in Sec. IV and compared with the results of the SPA of Sec. II and also with the results of the SPA performed on the cleavage formula for the coupling. Finally, in Sec. V we present our conclusions.

II. STATIONARY PHASE APPROXIMATION FORMULA FOR THE EXCHANGE COUPLING IN A Co/Cu/Co(001) TRILAYER

We consider N (001) planes of Cu with the bulk lattice constant sandwiched between two semi-infinite slabs of ferromagnetic fcc Co. A small lattice mismatch between Co and Cu is neglected. Following our original approach,[5,6] we assume that the local potentials in the Cu and Co layers are frozen, i.e., they do not change in going from the AF to the FM configuration of the trilayer. As discussed in the Introduction, this is equivalent to the force theorem. It follows that the exchange coupling per surface atom is given in terms of the thermodynamic potentials Ω^{σ} for electrons of spin σ by

$$J(N)=[\Omega^{\uparrow}(N)+\Omega^{\downarrow}(N)]_{\mathrm{FM}}-[\Omega^{\uparrow}(N)+\Omega^{\downarrow}(N)]_{\mathrm{AF}}. \quad (1)$$

The thermodynamic potential per surface atom for a given magnetic configuration at temperature T is given by

$$\Omega^{\sigma}=-\frac{k_BT}{N_{\parallel}}\sum_{\vec{k}_{\parallel}}\int_{-\infty}^{+\infty}\ln\{1+\exp[(\mu-E)/k_BT]\}\times\mathcal{D}^{\sigma}(E,\vec{k}_{\parallel},N)dE, \tag{2}$$

where $N_{\parallel}$ is the number of atoms in any atomic plane parallel to the layer structure, μ is the chemical potential, and $\mathcal{D}^{\sigma}$ is the spectral density for particles of spin σ in the trilayer having that configuration. Because of the in-plane translational invariance, we label all the trilayer states by the plane index i and by the wave vector $\vec{k}_{\parallel}$ parallel to the layers. The spectral density $\mathcal{D}^{\sigma}$ is given by

$$\mathcal{D}^{\sigma}(E,\vec{k}_{\parallel},N)=-\frac{1}{\pi}\mathrm{Im\ Tr}\sum_{i}G_{ii}^{\sigma}(E,\vec{k}_{\parallel},N), \tag{3}$$

where G_{ii}^{σ} is the diagonal matrix element of the tight-binding one-electron Green's function, the trace is over all atomic orbitals, and the sum over i is over all atomic planes in the trilayer. In this section, we restrict the sum over i to the atomic planes in the Cu spacer layer. The advantage of using the spectral density in the Cu spacer only is that it allows a transparent physical interpretation of the coupling in terms of the band structures of bulk Cu and Co. Moreover, the coupling can also be easily linked to photoemission experiments.[10–12] The numerical calculation of Sec. IV will allow us to assess the accuracy of this approximation.

The problem now reduces to the calculation of the spectral density and evaluation of the difficult $\vec{k}_{\parallel}$ and energy sums. We showed for a single-orbital model with complete confinement that both the $\vec{k}_{\parallel}$ and energy sums can be evaluated analytically using the stationary-phase approximation.[5] We need to generalize the method to a Co/Cu(001) trilayer. The generalization is based on the hypothesis[6] that, for large N, the normalized spectral density $(1/N)\Delta\mathcal{D}(E,\vec{k}_{\parallel},N)=(1/N)\{[\mathcal{D}^{\uparrow}+\mathcal{D}^{\downarrow}]_{\mathrm{FM}}-[\mathcal{D}^{\uparrow}+\mathcal{D}^{\downarrow}]_{\mathrm{AF}}\}$ is a periodic function of N. For periods incommensurate with the lattice, which is generally the case, the concept of a periodic function needs to be clarified. Although the physical spectral density is defined and can be computed only for integral numbers N of Cu atomic planes, we can consider formally its continuation to all real values of N. The continuation is a function that coincides with the physical spectral density when restricted to integers N. We shall say that the physical normalized spectral density is periodic in N provided its continuation is a periodic function. We show explicitly how to construct the continuation of the normalized spectral density for Co/Cu(001) and demonstrate that it is a periodic function.

Assuming that the normalized spectral density is periodic in N (for large N), we can expand it in a Fourier series. A rigorous proof of the periodicity in N is provided in Ref. 15. The exchange coupling then takes the form

$$J(N)=-\frac{k_BTN}{N_{\parallel}}\mathrm{Re}\sum_{s=1}^{\infty}\sum_{\vec{k}_{\parallel}}\int_{-\infty}^{+\infty}\ln\{1+\exp[(\mu-E)/k_BT]\}\times|\Delta c_s(E,\vec{k}_{\parallel})|e^{2i(sNk_{\perp}d+\psi_s)}dE, \tag{4}$$

where d is the interplanar distance, $|\Delta c_s(E,\vec{k}_{\parallel})|$ and $2\psi_s(E,\vec{k}_{\parallel})$ are the modulus and phase of the Fourier coefficients of the normalized spectral density $(1/N)\Delta\mathcal{D}(E,\vec{k}_{\parallel},N)$, and $\pi/k_{\perp}(E,\vec{k}_{\parallel})$ is its period. It is shown in Ref. 15 that $k_{\perp}(E,\vec{k}_{\parallel})$ is the wave vector perpendicular to the (001) plane obtained by solving the bulk Cu dispersion $E=E(\vec{k}_{\parallel},k_{\perp})$.

Expression (4) for the coupling is now in a form to which the SPA method can be readily applied.[5,6] For large N and any fixed energy E, the imaginary exponential in Eq. (4) oscillates rapidly as a function of $\vec{k}_{\parallel}$ and nonzero contributions to the $\vec{k}_{\parallel}$ integral come only from the neighborhood of points $\vec{k}_{\parallel}^{0}$ in $\vec{k}_{\parallel}$ space at which $k_{\perp}(E,\vec{k}_{\parallel})$ is stationary. The perpendicular wave vector $k_{\perp}(E,\vec{k}_{\parallel})$ in the argument of the exponential is expanded in a Taylor series about $\vec{k}_{\parallel}^{0}$ up to second order in $\vec{k}_{\parallel}$ and all the other factors depending on $\vec{k}_{\parallel}$ are approximated by their values at the extremal point $\vec{k}_{\parallel}^{0}$. The remaining integrals in $\vec{k}_{\parallel}$ space can be reduced to Gaussian integrals and evaluated analytically. The procedure is standard,[5] the only new feature is the presence of the phase ψ_s in the argument of the exponential function in Eq. (4). In general, ψ_s is nonzero. We can either treat ψ_s along with $|\Delta c_s(E,\vec{k}_{\parallel})|$ as a slowly varying function of $\vec{k}_{\parallel}$ and approximate ψ_s by its value at the stationary point or we can expand ψ_s in a Taylor series and include its dependence on $\vec{k}_{\parallel}$ in the Gaussian integrals. In the latter case, we would obtain a correction to the phase of the exchange coupling $\propto 1/N$ that is negligible in the asymptotic limit of large N. We shall, therefore, approximate ψ_s in the evaluation of the $\vec{k}_{\parallel}$ integral by its value at the stationary point.

The energy integral in Eq. (4) can also be evaluated analytically for large N. We recall[5] that, having made the stationary-phase approximation in the $\vec{k}_{\parallel}$ integral, we are left with an imaginary exponential $e^{2i[sNk_{\perp}d(E,\vec{k}_{\parallel}^{0})+\psi_s(E,\vec{k}_{\parallel}^{0})]}$ in the energy integral. For large N the exponential oscillates rapidly as a function of E. This results in cancellations and the only contribution to the energy integral thus comes from energies in the vicinity of the chemical potential μ at which the integral terminates abruptly.[5] Formally, one expands the argument of the exponential up to first order in E and the resultant integral is evaluated in the complex plane.[5] Again we have two options in dealing with the energy dependence of the phase. Either we approximate $\psi_s(E,\vec{k}_{\parallel}^{0})$ by its value at $E=\mu$ or expand it about μ together with $k_{\perp}(E,\vec{k}_{\parallel}^{0})$. It is now prudent to adopt the second option because an energy dependence of ψ_s leads no longer to a mere phase shift but may alter the decay of the coupling with N as well as its temperature dependence.[28] Treating the energy dependence of the phase ψ_s on the same footing as the energy dependence of $k_{\perp}$,[5] it is straightforward to derive the following asymptotic formula for the exchange coupling $J(N)$:

$$J=\mathrm{Re}\sum_{\vec{k}_{\parallel}^{0}}\sum_{s=1}^{\infty}\frac{\tau}{2s}\frac{|\Delta c_s|e^{2i(sNk_{\perp}d+\psi_s)}}{2\left(sNd\dfrac{\partial k_{\perp}}{\partial E}+\dfrac{\partial\psi_s}{\partial E}\right)}\times\frac{k_BTd\left|\dfrac{\partial^2k_{\perp}}{\partial k_x^2}\dfrac{\partial^2k_{\perp}}{\partial k_y^2}\right|^{-1/2}}{\sinh\left[2\pi k_BT\left(sNd\dfrac{\partial k_{\perp}}{\partial E}+\dfrac{\partial\psi_s}{\partial E}\right)\right]}, \tag{5}$$

where k_x, k_y are the components of $\vec{k}_\parallel$ in an orthogonal system of axes chosen to diagonalize the Taylor expansion of the argument of the exponential in Eq. (4). The sum over $\vec{k}_\parallel^0$ covers all the stationary points of $k_\perp$, $\tau = i$ when both second derivatives in Eq. (4) are positive, $\tau = -i$ when they are negative, and $\tau = 1$ when the derivatives have opposite signs. The perpendicular wave vector $k_\perp$, Fourier coefficients Δc_s, and all the derivatives in Eq. (5) are evaluated at $E = \mu$ and at the stationary point $\vec{k}_\parallel = \vec{k}_\parallel^0$. It should be noted that, for $\partial \psi_s / \partial E = 0$, Eq. (5) reduces exactly to the asymptotic formula for the coupling derived in Ref. 7.

We begin the evaluation of Eq. (5) for Co/Cu(001) with the factors that depend only on the bulk Cu Fermi surface (FS) (the difference between μ and E_F is negligible in the relevant range of temperatures). They are the oscillation periods, curvatures of the Cu FS, and ''inverse FS velocities'' $\partial k_\perp / \partial E$. The oscillation periods $\pi / k_\perp^0$ were obtained from the Cu FS extremal radii in the [001] direction. There are two extremal radii $k_\perp^0$ and they occur for $\vec{k}_\parallel^b = (0,0)$ (belly) and $\vec{k}_\parallel^n a = (\pm 2.53, \pm 2.53)$ (necks) where $a = 3.6$ Å is the lattice constant of Cu. The corresponding periods are $p^b = 5.7$ atomic planes (~ 10.3 Å) and $p^n = 2.6$ atomic planes (~ 4.7 Å), respectively. The factor $\tau = i$ for the belly and $\tau = 1$ for the necks. The Cu FS curvatures $|(\partial^2 k_\perp / \partial k_x^2)(\partial^2 k_\perp / \partial k_y^2)|^{-1/2}$ and inverse FS velocities $\partial k_\perp / \partial E$ at the belly and neck extrema were determined using a tight-binding parametrization[29] of the first-principles band structure of bulk Cu. Their values for the belly are $|(\partial^2 k_\perp / \partial k_x^2)(\partial^2 k_\perp / \partial k_y^2)|^{-1/2} = 0.393$ (Å)$^{-1}$, $\partial k_\perp / \partial E = -1.583$ (Ry Å)$^{-1}$. The corresponding values for the necks are $|(\partial^2 k_\perp / \partial k_x^2)(\partial^2 k_\perp / \partial k_y^2)|^{-1/2} = 0.298$ (Å)$^{-1}$, $\partial k_\perp / \partial E = 2.057$ (Ry Å)$^{-1}$.

The last ingredient in Eq. (5) is the Fourier analysis of the normalized spectral density $(1/N)\Delta \mathcal{D}(E, \vec{k}_\parallel, N)$. We first computed the spectral densities for both spin orientations in the FM and AF configurations for discrete (physical) values of the Cu thickness $L = Nd$. The required Green's functions were calculated within the tight-binding model with s, p, and d orbitals, and hopping to first- and second-nearest neighbors. The tight-binding parameters for all Cu planes were determined from the best fit to the first-principles band structure[29] of bulk Cu. The parameters for fcc ferromagnetic Co were obtained starting from paramagnetic[29] Co and adjusting self-consistently the on-site energies to get the best agreement with the first-principles band structure[30] of fcc ferromagnetic Co. At the Co/Cu interface, the Cu hopping parameters were used and the reason for this choice is discussed in Sec. IV. Using these values of the tight-binding parameters, we constructed the 18×18 Hamiltonian matrix $H(\vec{k}_\parallel)$ of a principal layer[31] consisting of two (001) atomic planes of Cu (Co). The Cu and Co principal layers are introduced because the Hamiltonian of a Co/Cu trilayer with arbitrary numbers of Cu and Co planes can be obtained by stacking the appropriate sequence of principal layers with hopping only between the neighboring principal layers. Using the method of adlayers,[32] we first determined recursively the local Green's function in the surface layer of a stack of Cu principal layers deposited on a semi-infinite stack of Co principal layers. Principal layers of Cu were deposited one by one from left to right and the surface Green function was updated from the Dyson equation after each deposition. If $g_{\rm old}^\sigma$ and $g_{\rm new}^\sigma$ denote, respectively, the 18×18 surface Green's function matrices before and after deposition of a single principal layer, then the basic recursion step is

$$[g_{\rm new}^\sigma]^{-1} = [g_{\rm isol}^\sigma]^{-1} - t^\dagger(\vec{k}_\parallel) g_{\rm old}^\sigma t(\vec{k}_\parallel), \tag{6}$$

where $g_{\rm isol}^\sigma$ is the Green's function for an isolated principal layer of Cu, $t(\vec{k}_\parallel)$ is the hopping matrix between two neighboring principal layers, and we suppress for brevity E and $\vec{k}_\parallel$ in the arguments of the Green's functions. The method of adlayers yields with machine accuracy the Green's function matrix $g_\swarrow^\sigma(j)$ in the surface principal layer of the left overlayer of j principal layers of Cu on semi-infinite Co. Similarly, we obtained the surface Green's function $g_r^\sigma(N/2 - j)$ for the right overlayer of $N/2 - j$ principal layers of Cu on semi-infinite Co (if the number N of Cu atomic planes is odd, we first deposit a single atomic plane of Cu and then proceed with principal layers). Finally, we completed the trilayer by switching on the hopping $t(\vec{k}_\parallel)$ between the left and right overlayers. The exact Green's function in the principal layer j next to the joint obtained from Dyson's equation[32] is given by

$$[G^\sigma(j)]^{-1} = [g_r^\sigma(N/2 - j)]^{-1} - t^\dagger(\vec{k}_\parallel) g_\swarrow^\sigma(j) t(\vec{k}_\parallel), \tag{7}$$

where we use the convention that capital letters denote Green's functions of the connected system and lower-case letters those of the cleaved system. The matrix elements of the Green's function in every atomic plane of Cu were determined by this method and the spectral density was calculated from Eq. (3). The only input in the adlayer procedure is the surface Green's function for semi-infinite Co that was determined by the decimation method of Ref. 33.

With the normalized spectral densities computed for integer N we can address the question of their continuation from discrete Cu thickness $L = Nd$ to all real values of L. We require for the Fourier analysis the knowledge of the spectral density for all values of the ''continuous Cu thickness'' L in the interval $(-\pi/2k_\perp, \pi/2k_\perp)$, where $k_\perp$ is either the belly or neck FS radius. We first generated the spectral densities for trilayers with the number of Cu atomic planes N ranging up to 600. The spectral densities normalized to N were then shifted to the first period $(-\pi/2k_\perp, \pi/2k_\perp)$ by subtracting from N the appropriate integral number of periods $\pi/k_\perp$. If all the shifted points condense, as we anticipate, on a continuous curve then this test demonstrates that the normalized spectral density is asymptotically a periodic function of the continuous Cu thickness L with a period $\pi/k_\perp$. At the same time, the shifting algorithm provides us with a dense set of points in the interval $(-\pi/2k_\perp, \pi/2k_\perp)$, which can be Fourier analyzed with any required accuracy. An alternative method of calculating the spectral density as a continuous function of the layer thickness, which has been developed by Umerski,[15] is discussed briefly in Sec. III.

One of the main advantages of the stationary-phase method discussed here is that it permits an explicit separation of the contributions to the exchange coupling arising from different extrema of the Cu Fermi surface. This is the only method available up to now in which the contributions from

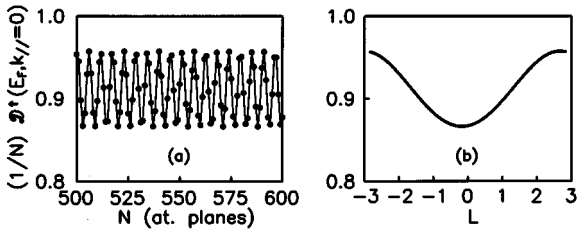

FIG. 1. (a) Computed normalized spectral density at the Fermi energy and $\vec{k}_{\parallel}=0$ (belly) for the majority electrons in the FM configuration. (b) Normalized spectral density for the majority-spin electrons in the FM configuration shifted to the first period $(-\pi/2k_{\perp},\pi/2k_{\perp})$.

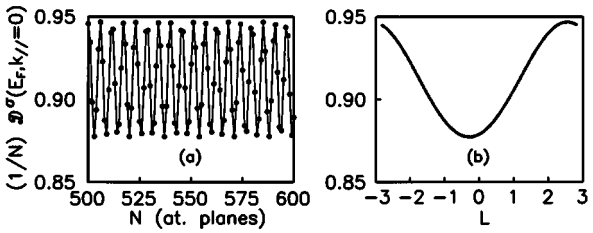

FIG. 3. (a) Computed normalized spectral density at the Fermi energy and $\vec{k}_{\parallel}=0$ (belly) for electrons of either spin orientation in the AF configuration. (b) Normalized spectral density for the majority/minority electrons in the AF configuration shifted to the first period $(-\pi/2k_{\perp},\pi/2k_{\perp})$.

the neck and belly extrema can be separated rigorously. We start with the long-period component that originates from the belly extremum. The raw spectral densities $(1/N)\mathcal{D}^{\sigma}(E_F,\vec{k}_{\parallel}=0,N)$ computed for the FM and AF configurations are shown in Figs. 1(a), 2(a), and 3(a) together with the data shifted to the first period [Figs. 1(b), 2(b), and 3(b)]. As anticipated, all three normalized spectral densities are strictly periodic with the same period $p^b=5.7$ atomic planes and their oscillations as a function of the Cu thickness reflect the passage across the Fermi surface of resonant electron states partially confined in the Cu slab by the spin-dependent Co potentials. By comparing the shifted spectral densities for different values of the energy, we checked that the energy dependence of the phase ψ_s is negligibly weak $(\partial\psi_1/\partial E\simeq 0.3\ \mathrm{Ry}^{-1}$ for the fundamental oscillation $s=1)$.

The amplitude of each component of the normalized spectral density is determined by the degree of confinement of electron states in Cu, which can be judged from the offsets of the bulk Cu and Co bands along the Γ-X line $(\vec{k}_{\parallel}=0)$ shown in Fig. 4. The relevant sp-like band intersecting the Cu Fermi level matches quite well the corresponding majority and minority bands in Co, which results in a weak magnetic contrast. The corresponding coupling amplitude is, therefore, very small. This is illustrated in Fig. 5, which shows the long-period belly contribution to the coupling obtained from Eq. (5) at room (solid circles) and zero (squares) temperatures. The left-hand scale in Fig. 5 gives the coupling in mRy per atom in the (001) surface. The right-hand scale gives the conversion to the units $(\mathrm{mJ/m}^2)$ commonly used by experimentalists. The contribution to the coupling from the Cu FS belly is clearly far too weak to account for the total observed[34] coupling strength of about 0.4 $\mathrm{mJ/m}^2$. It is also clear from Fig. 5 that the belly contribution to the coupling hardly changes from zero to room temperature. This is because the temperature dependence in this case is determined entirely by the inverse Fermi surface velocity $\partial k_{\perp}/\partial E$. The contribution of the term $\partial\psi_s/\partial E$ is negligible.

We now turn to the short-period neck contribution, which is much more interesting. Examination of all three components of the shifted spectral density shown in Fig. 6 reveals that carriers of both spin orientations in the AF configuration [Fig. 6(a)], and also the majority spin carriers in the FM configuration [Fig. 6(b)], are only weakly confined (broad resonances). However, the minority spin carriers become completely confined in a quantum well in the FM configuration. As far as we can determine numerically, their spectral density is a periodic sequence of δ functions which, when shifted to the first period, has the form shown in Fig. 6(c). [The peak in Fig. 6(c) has nonzero width because a small imaginary part is added to the energy in the decimation method.] To explain the physical origin of the complete confinement we reproduce in Fig. 7 the band structures of bulk Cu and Co in the relevant [001] direction for one of the neck wave vectors, $\vec{k}_{\parallel}^{n}a=(2.53,2.53)$. The sp-like Cu band that intersects the Fermi level in Cu, and hence determines the coupling, has no counterpart for the minority spin in Co since it falls into a hybridization gap. The minority-spin carriers must, therefore, be fully confined in Cu in the FM configuration. On the other hand, there is an sp-like Co majority-spin band intersecting the Fermi level into which

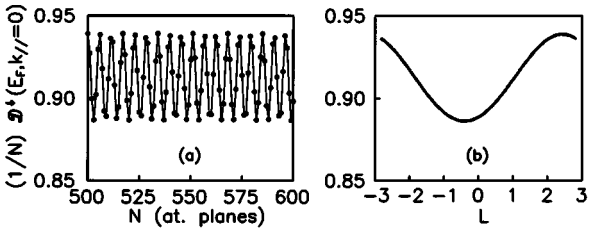

FIG. 2. (a) Computed normalized spectral density at the Fermi energy and $\vec{k}_{\parallel}=0$ (belly) for the minority electrons in the FM configuration. (b) Normalized spectral density for the minority-spin electrons in the FM configuration shifted to the first period $(-\pi/2k_{\perp},\pi/2k_{\perp})$.

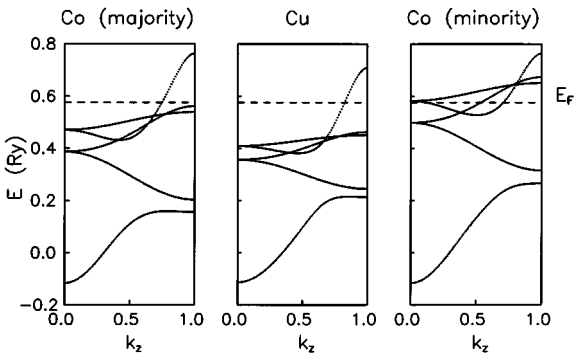

FIG. 4. Band structures of Cu and ferromagnetic fcc Co along the Γ-X line $(\vec{k}_{\parallel}=0)$.

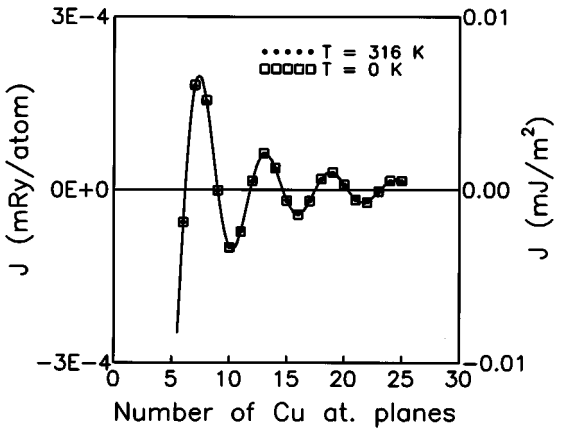

FIG. 5. Long-period (belly) contribution to the coupling obtained from Eq. (5) at room (full circles) and zero (squares) temperatures. The left-hand scale gives the coupling in mRy per atom in the (001) surface, the right-hand scale in mJ/m^2.

the corresponding Cu band can evolve. The confinement of the majority-spin carriers is, therefore, only partial. Because of this asymmetry in the confinement of the majority and minority carriers, the magnetic contrast is very large and we expect strong coupling.

However, there is another interesting feature of the full confinement at the neck which influences the coupling strength. We refer here to a very strong energy dependence of the phase ψ_s for minority carriers in the FM configuration and for carriers of either spin orientation in the AF configuration. First of all, we note that, in both these cases, the Fourier analysis of the spectral density at the neck shows that $\psi_s \approx s\psi$, where ψ is universal. It follows that only the energy dependence of ψ is required. We determined it numerically from the shifted spectral density. We now discuss separately the behavior of ψ for the minority and majority carriers in the FM and AF configurations. The results for the minority carriers, which are confined in the FM configuration, are shown in Fig. 8. The energy dependence of the phase $\psi^{\downarrow}_{\mathrm{FM}}$ is almost linear which means that the derivative $\partial(\psi^{\downarrow})_{\mathrm{FM}}/\partial E$ required in Eq. (5) can be determined very accurately. We find $\partial(\psi^{\downarrow})_{\mathrm{FM}}/\partial E = -59\ \mathrm{Ry}^{-1}$ for the minority carriers in the FM configuration. Similarly, $\partial(\psi^{\downarrow,\uparrow})_{\mathrm{AF}}/\partial E = -29\ \mathrm{Ry}^{-1}$ in the AF configuration when carriers of either spin orientation are confined at only one of the interfaces. (The energy dependence of the phase for the majority carriers weakly confined in the FM configuration is again negligible.) To visualize the effect of these large values of $\partial\psi/\partial E$ on the coupling strength, it is useful to note from Eq. (5) that it is formally equivalent to adding a fixed number $(sd\partial k_{\perp}/\partial E)^{-1}\partial\psi_s/\partial E$ of about 20 atomic planes of Cu to the nominal thickness of the Cu slab. The coupling strength is, therefore, greatly reduced for small Cu thickness and deviates strongly from the $1/N^2$ law that usually holds at $T=0$. Full discussion of this anomalous behavior of the coupling strength is deferred to Sec. IV.

The temperature dependence of the coupling is also strongly influenced by the rapid variation of the phase ψ with energy.[28] The contribution to the coupling from the four necks of the Cu FS obtained from Eq. (5) at room (solid curve) and zero (dashed curve) temperatures is shown in Fig. 9. Virtually all of the change of the coupling strength between zero and room temperature shown in Fig. 9 is due to the strong energy dependence of the phase ψ. This is in contrast to the belly contribution for which this effect is negligible.

Finally, comparison of the belly (Fig. 5) and neck (Fig. 9) contributions to the total coupling shows that the exchange coupling in a Co/Cu(001) trilayer with thick Co layers is totally dominated by the short-period (neck) oscillation.

III. CLEAVAGE FORMULA FOR THE EXCHANGE COUPLING IN MAGNETIC MULTILAYERS

The numerical effort needed to evaluate the coupling in a Co/Cu trilayer from the stationary-phase formula (5) is minimal. This is because the sum of the spectral densities in all the Cu atomic planes is required only for two values of $\vec{k}_{\parallel}$ (belly and neck) and one value of the energy ($E=E_F$). However, if one were to evaluate the coupling numerically from Eq. (2) as it stands, the numerical effort would be prohibitive. Moreover, the accuracy of the approximation of Sec. II, which includes only the spectral density in the Cu spacer layer, needs to be tested. We have, therefore, derived a new cleavage formula for the coupling which not only can be evaluated numerically much more efficiently but also includes explicitly the contribution to the coupling from all the atomic planes in an infinite layer structure. Historically, the cleavage formula was obtained by introducing the cleavage-plane formalism[25] of the spin-current (torque) approach[26] in the formulation of d'Albuquerque Castro, Ferreira, and Muniz.[27] We first present this original derivation and then describe an alternative method in which the cleavage formula is obtained by summing directly the spectral density in

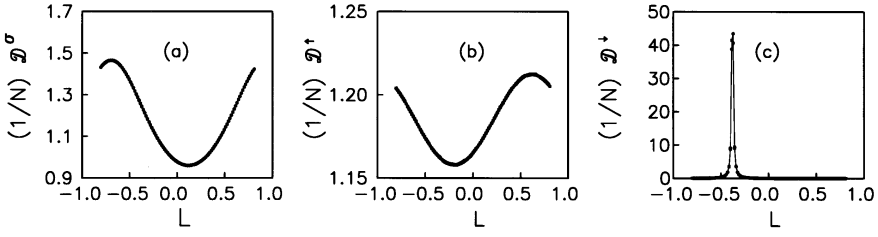

FIG. 6. Shifted normalized spectral densities at E_F and $\vec{k}_{\parallel}a=(2.53,2.53)$ (neck). (a) Carriers of either spin orientation in the AF configuration; partial confinement. (b) Majority-spin carriers in the FM configuration; partial confinement. (c) Minority-spin carriers in the FM configuration; full confinement.

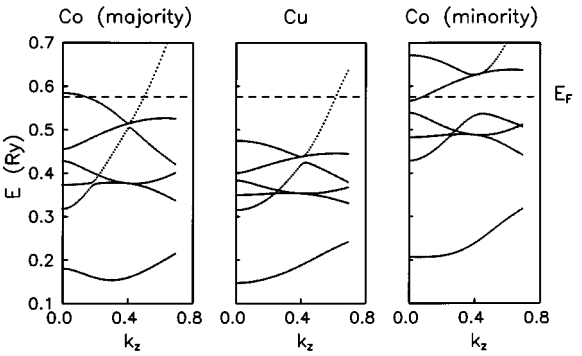

FIG. 7. Band structures of Cu and fcc Co in the relevant [001] direction for one of the necks [$\vec{k}_\parallel a=(2.53,2.53)$].

all the atomic planes. For simplicity, we restrict our derivation to the case of nearest-neighbor hopping only. Hopping to more distant neighbors is trivially dealt with by using the technique of principal layers[31] described in Sec. II.

We begin by considering a more general system consisting of two ferromagnetic layers, with M atomic planes each, embedded in a nonmagnetic material. The two magnetic layers are separated by N atomic planes of the nonmagnetic material, and are labeled A and B. The atomic planes in each magnetic layer are labeled m and m', respectively ($1\leqslant m\leqslant M$; $M+N+1\leqslant m'\leqslant 2M+N$). According to Eq. (1), the coupling J is defined as the change in the thermodynamic potential Ω of the system when the magnetization in one of the layers is rotated by π relative to that in the other layer,

$$J=\Delta\Omega(\pi)=\Omega(0)-\Omega(\pi). \tag{8}$$

For an arbitrary angle of rotation θ in the plane of the layers, the change in Ω can be written as[27]

$$\Delta\Omega(\theta)=-\frac{1}{N_\parallel\pi}\sum_{\vec{k}_\parallel}\int dE f(E)\,\mathrm{Im\ Tr\ ln}\{1-2(\cos\theta-1)\times\mathbf{V}_{\mathrm{ex}}\mathbf{G}^{\uparrow}_{B,A}(E,\vec{k}_\parallel)\mathbf{V}_{\mathrm{ex}}\mathbf{G}^{\downarrow}_{A,B}(E,\vec{k}_\parallel)\}, \tag{9}$$

where $f(E)$ is the Fermi-Dirac distribution function and the trace (Tr) is over all the atomic orbitals. The matrix

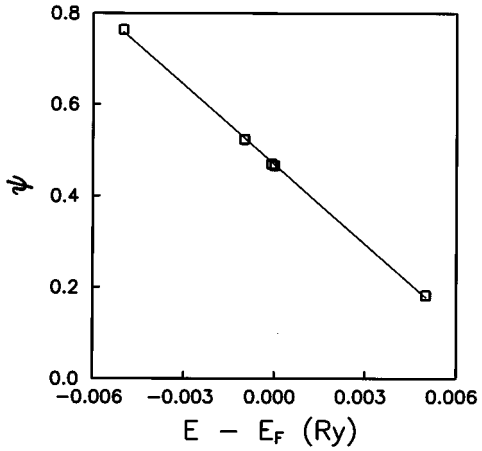

FIG. 8. Energy dependence of the phase ψ of the Fourier coefficients for the minority carriers in the FM configuration at the neck extremum.

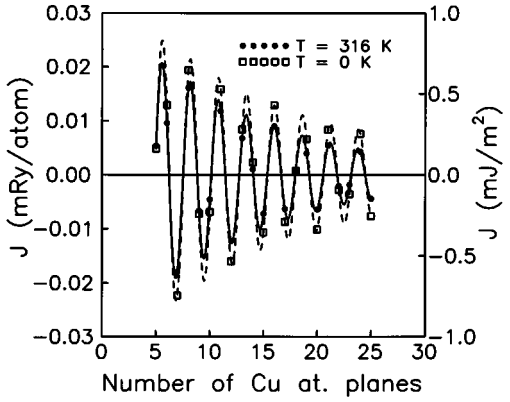

FIG. 9. Contribution to the exchange coupling of the four neck extrema of the Cu Fermi surface at room (solid curve) and zero (dashed curve) temperatures.

$\mathbf{G}^{\uparrow}_{Bm',Am}$ ($\mathbf{G}^{\downarrow}_{Am,Bm'}$) is the propagator for an up-spin (down-spin) electron between every atomic plane m' (m) in block B (A) and every atomic plane m (m') in block A (B). We stress that A and B are just labels for the left and right ferromagnets, *not* indices. Here, $\mathbf{V}_{\mathrm{ex}}$ is a block-diagonal matrix. Each block of $\mathbf{V}_{\mathrm{ex}}$ is a $\nu\times\nu$ matrix (ν is the number of atomic orbitals in the tight-binding basis) whose elements are given by the on-site Hartree-Fock exchange energies in each magnetic layer. Note that the dimension of the matrices $\mathbf{G}^{\uparrow}_{B,A}$, $\mathbf{G}^{\downarrow}_{A,B}$, and $\mathbf{V}_{\mathrm{ex}}$ is equal to $(M\nu)\times(M\nu)$. The large size of these matrices for thick ferromagnetic layers makes it impractical to use Eq. (9) as it stands. However, it is possible to reformulate Eq. (9) in terms of matrices whose sizes depend just on ν. Following Edwards, Robinson, and Mathon,[25] we separate the multilayer system into two independent parts, referred to as left (ℓ) and right (r) overlayers, by introducing a cleavage plane between spacer planes j and $j+1$. The left overlayer consists of j atomic planes of Cu deposited on a substrate consisting of semi-infinite Cu and M atomic planes of Co. The right overlayer consists of $N-j$ atomic planes of Cu deposited on a similar substrate. Formally, if the planes j and $j+1$ are coupled by a hopping matrix t, then the Hamiltonian H for the whole system can be split into two terms, $H=h+\Delta h$. Here, h is a block-diagonal matrix that describes the two semi-infinite cleaved systems obtained from H by setting the hopping t between planes j and $j+1$ equal to zero and Δh is defined by

$$\Delta h_{p,q}\equiv\begin{cases} t, & p=j, \quad q=j+1 \\ t^{\dagger}, & p=j+1, \quad q=j \\ 0, & \text{otherwise.}\end{cases} \tag{10}$$

As in Sec. II, we use the convention that capital letters describe the whole connected system, while lower case letters are reserved for the semi-infinite cleaved system. In addition, we use boldface letters to denote matrices whose dimension depends on the ferromagnet thickness M.

Using Dyson's equation, we can relate the Green's functions of the connected system to the surface Green's functions of the cleaved system

$$\mathbf{G}^{\uparrow}_{Bm',Am}=\mathbf{g}^{\uparrow}_{Bm',j+1}t^{\dagger}(I-g^{\uparrow}_{j,j}tg^{\uparrow}_{j+1,j+1}t^{\dagger})^{-1}\mathbf{g}^{\uparrow}_{j,Am} \tag{11}$$

and

$$\mathbf{G}^{\downarrow}_{Am,Bm'}=\mathbf{g}^{\downarrow}_{Am,j}t(I-g^{\downarrow}_{j+1,j+1}t^{\dagger}g^{\downarrow}_{j,j}t)^{-1}\mathbf{g}^{\downarrow}_{j+1,Bm'}, \quad (12)$$

where the unit matrix I and the matrices $t, g^{\sigma}_{j,j}, g^{\sigma}_{j+1,j+1}$ are all $\nu\times\nu$ matrices. The matrices $\mathbf{g}^{\downarrow}_{Am,j}$ and $\mathbf{g}^{\uparrow}_{Bm',j+1}$ have dimension $(M\nu)\times\nu$, while $\mathbf{g}^{\uparrow}_{j,Am}$ and $\mathbf{g}^{\downarrow}_{j+1,Bm'}$ are $\nu\times(M\nu)$. The matrices $g^{\sigma}_{j,j}$ and $g^{\sigma}_{j+1,j+1}$ are, respectively, equal to $g^{\sigma}_{\nearrow}(j)$ and $g^{\sigma}_{r}(N-j)$ defined in Sec. II. We now introduce the $\nu\times\nu$ matrices $S^{\uparrow}=t^{\dagger}(\vec{k}_{\parallel})[I-g^{\uparrow}_{\nearrow}t(\vec{k}_{\parallel})g^{\uparrow}_{r}t^{\dagger}(\vec{k}_{\parallel})]^{-1}$ and $S^{\downarrow}=t(\vec{k}_{\parallel})[I-g^{\downarrow}_{r}t^{\dagger}(\vec{k}_{\parallel})g^{\downarrow}_{\nearrow}t(\vec{k}_{\parallel})]^{-1}$, and write the argument of the logarithmic function in Eq. (9) as

$$\begin{aligned}&\mathrm{Tr}\ \ln\{I-2(\cos\theta-1)\mathbf{V}_{\mathrm{ex}}\mathbf{g}^{\uparrow}_{B,j+1}S^{\uparrow}\mathbf{g}^{\uparrow}_{j,A}\mathbf{V}_{\mathrm{ex}}\,\mathbf{g}^{\downarrow}_{A,j}S^{\downarrow}\mathbf{g}^{\downarrow}_{j+1,B}\}\\&\quad=\mathrm{Tr}\ \ln\{I-2(\cos\theta-1)S^{\uparrow}\mathbf{g}^{\uparrow}_{j,A}\mathbf{V}_{\mathrm{ex}}\mathbf{g}^{\downarrow}_{A,j}S^{\downarrow}\mathbf{g}^{\downarrow}_{j+1,B}\\&\qquad\times\mathbf{V}_{\mathrm{ex}}\mathbf{g}^{\uparrow}_{B,j+1}\}. \quad (13)\end{aligned}$$

We make use of Dyson's equation again to write

$$2\mathbf{g}^{\uparrow}_{j,A}\mathbf{V}_{\mathrm{ex}}\mathbf{g}^{\downarrow}_{A,j}=g^{\downarrow}_{\nearrow}-g^{\uparrow}_{\nearrow} \quad (14)$$

and

$$2\mathbf{g}^{\downarrow}_{j+1,B}\mathbf{V}_{\mathrm{ex}}\mathbf{g}^{\uparrow}_{B,j+1}=g^{\uparrow}_{r}-g^{\downarrow}_{r}. \quad (15)$$

By substituting these results into Eqs. (13), (9), and (8) we end up with the following expression for J:

$$J=\frac{1}{N_{\parallel}}\sum_{\vec{k}_{\parallel}}\int dE f(E)F(\vec{k}_{\parallel},E,N), \quad (16)$$

where

$$F=-\frac{1}{\pi}\mathrm{Im}\ \mathrm{Tr}\ \ln[I+S^{\uparrow}(g^{\uparrow}_{\nearrow}(j)-g^{\downarrow}_{\nearrow}(j))\times S^{\downarrow}(g^{\uparrow}_{r}(N-j)-g^{\downarrow}_{r}(N-j))]. \quad (17)$$

It is worth stressing that the dimension of all matrices in Eq. (17) is determined by the number of atomic orbitals in the tight-binding basis and *does not* depend on the number of planes in the magnetic layers. The dependence of J on the magnetic layer thickness M is implicit and contained entirely in the surface Green's functions of the two cleaved systems. This makes it possible to calculate the coupling for large or even infinite values of M, which is prohibitive within other formalisms such as that of Lang *et al.*[20] The extension of the above expression to systems with magnetic layers of different thicknesses is straightforward. In addition, it can be easily shown that, for the single-band model, Eq. (17) reduces to the torque formula of Edwards, Robinson, and Mathon.[25] As in that case, it is easily shown that F is independent of the cleavage-plane position. In the torque formulation, this is an immediate consequence of the spin current conservation. Equation (17) has already been used in Refs. 14,13, and 28 and derived independently by Drchal *et al.*[19]

We now present an alternative derivation that shows much more directly how the cleavage formula for the coupling is related to the spectral density approach of Sec. II. In fact, we are going to derive the cleavage formula from Eq. (3) of Sec. II by summing explicitly over all the atomic planes of the system. As before, we use the notation $g^{\sigma}_{p,q}$ for the matrix elements of the one-electron Green's function of the cleaved system and $G^{\sigma}_{p,q}$ for those of the connected multilayer.

To evaluate the spectral density from Eq. (3), we require the diagonal elements of the connected Green's function $G^{\sigma}_{p,p}$ in all the atomic planes of the system. We once again cleave our system between the jth and $j+1$th layers. Using Dyson's equation, we can express them in terms of the Green's-function elements of the cleaved system $g_{p,q}$,

$$G^{\sigma}_{p,p}=\begin{cases}g^{\sigma}_{p,p}+g^{\sigma}_{p,j}t(I-g^{\sigma}_{j+1,j+1}t^{\dagger}g^{\sigma}_{j,j}t)^{-1}g^{\sigma}_{j+1,j+1}t^{\dagger}g^{\sigma}_{j,p} & \text{for } -\infty<p\leqslant j\\ g^{\sigma}_{p,p}+g^{\sigma}_{p,j+1}t^{\dagger}g^{\sigma}_{j,j}t(I-g^{\sigma}_{j+1,j+1}t^{\dagger}g^{\sigma}_{j,j}t)^{-1}g^{\sigma}_{j+1,p} & \text{for } j+1\leqslant p<\infty,\end{cases} \quad (18)$$

where I is again a $\nu\times\nu$ unit matrix and we have suppressed the dependence of all the Green's functions on E, $\vec{k}_{\parallel}$, and orbital indices. Substituting from Eq. (18) in Eq. (3), we can write the total spectral density of the connected system in a given configuration of the magnetic layers in terms of the Green's functions of the cleaved system,

$$\begin{aligned}\mathcal{D}^{\sigma}(N)=-\frac{1}{\pi}\mathrm{Im}\ \mathrm{Tr}\Bigg\{&\sum_{p=-\infty}^{j}[g^{\sigma}_{p,p}+g^{\sigma}_{p,j}t\\&\times(I-g^{\sigma}_{j+1,j+1}t^{\dagger}g^{\sigma}_{j,j}t)^{-1}g^{\sigma}_{j+1,j+1}t^{\dagger}g^{\sigma}_{j,p}]\\&+\sum_{p=j+1}^{\infty}[g^{\sigma}_{p,p}+g^{\sigma}_{p,j+1}t^{\dagger}g^{\sigma}_{j,j}t\\&\times(I-g^{\sigma}_{j+1,j+1}t^{\dagger}g^{\sigma}_{j,j}t)^{-1}g^{\sigma}_{j+1,p}]\Bigg\}. \quad (19)\end{aligned}$$

Now we use the identities $dg^{\sigma}_{j,j}/dE=-\Sigma^{\infty}_{p=-\infty}g^{\sigma}_{j,p}g^{\sigma}_{p,j}=-\Sigma^{j}_{p=-\infty}g^{\sigma}_{j,p}g^{\sigma}_{p,j}$ and $dg^{\sigma}_{j+1,j+1}/dE=-\Sigma^{\infty}_{p=-\infty}g^{\sigma}_{j+1,p}g^{\sigma}_{p,j+1}=-\Sigma^{\infty}_{p=j+1}g^{\sigma}_{j,p}g^{\sigma}_{p,j}$ to write the spectral density in the form

$$\begin{aligned}\mathcal{D}^{\sigma}(N)=&\mathcal{D}^{\sigma}_{\nearrow}(j)+\mathcal{D}^{\sigma}_{r}(N-j)\\&-\frac{1}{\pi}\mathrm{Im}\ \mathrm{Tr}\left(\frac{d}{dE}\ln(I-g^{\sigma}_{j+1,j+1}t^{\dagger}g^{\sigma}_{j,j}t)\right), \quad (20)\end{aligned}$$

where

$$\mathcal{D}^{\sigma}_{\nearrow}(j)=-\frac{1}{\pi}\mathrm{Im}\ \mathrm{Tr}\sum_{p=-\infty}^{j}g^{\sigma}_{p,p},$$

$$\mathcal{D}^{\sigma}_{r}(N-j)=-\frac{1}{\pi}\mathrm{Im}\ \mathrm{Tr}\sum_{p=j+1}^{\infty}g^{\sigma}_{p,p}$$

are simply the spectral densities for the left and right surface systems. Since they refer to the cleaved system, they are clearly independent of the magnetic configuration, and, hence, do not contribute to the coupling. The last term in Eq. (20), on the other hand, gives the difference between the spectral densities of the connected and cleaved systems. It is, therefore, this term that determines the exchange coupling. We note that it depends only on the surface Green's functions of the cleaved system.

We can now apply Eq. (20) to determine the coupling. An inspection of Eqs. (1)–(3) of Sec. II shows that we require the sum of the spectral densities for up- and down-spin carriers in the FM configuration and the spectral density of carriers of either spin in the AF configuration. In the FM configuration, an electron of spin σ moving across the cleavage plane obviously experiences the same potential in the left and right ferromagnets. To obtain the spectral density in the AF configuration, we note that, when the magnetizations of the Co layers are antiparallel, an electron with spin up in the left overlayer can be formally regarded as an electron with spin down in the right overlayer, and vice versa. This means that g_r^{σ} in Eq. (20) becomes $g_r^{\sigma'}$, where σ' is of opposite spin orientation to σ. We stress that this formal ''trick'' can only be used because our formulation is in terms of the Green's functions of a cleaved system; *no* physical spin flip actually takes place at the cleavage plane. It is now easy to obtain the difference $\Delta\mathcal{D}(N)$ between the spectral densities in the FM and AF configurations, bearing in mind that the surface terms cancel. It is given by

$$\Delta\mathcal{D}(N)=-\frac{1}{\pi}\mathrm{Im}\left(\frac{d}{dE}\ln[\det(R_{\uparrow\uparrow}R_{\downarrow\downarrow}R_{\uparrow\downarrow}^{-1}R_{\downarrow\uparrow}^{-1})]\right),$$

where

$$R_{\sigma,\sigma'}=(I-g_r^{\sigma'}t^{\dagger}g_{\nearrow}^{\sigma}t). \tag{21}$$

When the spectral density difference (21) is substituted in Eqs. (1) and (2), it is easy to check that the cleavage formula (17) for the coupling is recovered. For the purpose of tracing the contributions to the coupling of the majority and minority carriers in the FM and AF configurations separately, it is preferable to use Eq. (21) where these contributions can be clearly linked to the factors $R_{\uparrow\uparrow}$, $R_{\downarrow\downarrow}$, and $R_{\uparrow\downarrow}$.

In addition to the computational efficiency (particularly for thick magnetic layers) already referred to, the cleavage formula has an additional very important advantage that the two surface Green's functions $g_{\nearrow}^{\sigma}$ and g_r^{σ}, required in this formula, can be determined by a new essentially analytical method proposed recently by Umerski.[15] In his method, the adlaying procedure defined by Eq. (6) is reformulated using a matrix generalization of the bilinear mapping of the functions of a complex variable so that the thickness of an overlayer on a substrate appears explicitly as an independent variable in the overlayer Green's functions $g_{\nearrow}^{\sigma}$ and g_r^{σ}. It follows that one can treat formally the thickness of the overlayer and, hence the thickness of the spacer, as a continuous variable. The exchange coupling can, therefore, be calculated from Eqs. (16) and (17) entirely numerically for fractional values of the interplanar distance d. This method thus provides a dense set of points for the coupling that can be restricted to a relatively thin spacer. Such a dense set of computed data points can be reliably analyzed numerically for periods, amplitudes, and phases of all the oscillatory contributions to the coupling. This is, in particular, difficult when there are several oscillation periods. To achieve the same degree of accuracy with the conventional numerical methods, which give the coupling on discrete atomic planes only, one would have to go to very large spacer thicknesses where the convergence in the $\vec{k}_{\parallel}$ space becomes poor.

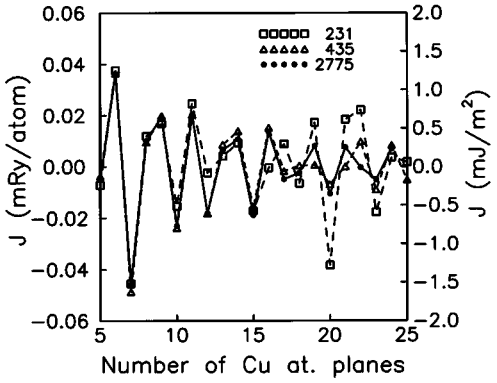

FIG. 10. Numerical evaluation of the exchange coupling for different numbers of points in the $\vec{k}_{\parallel}$ sum (squares, $N_{\parallel}=231$; triangles, $N_{\parallel}=435$; full circles, $N_{\parallel}=2775$).

IV. STATIONARY-PHASE APPROXIMATION TO THE CLEAVAGE FORMULA AND NUMERICAL EVALUATION OF THE EXCHANGE COUPLING IN Co/Cu/Co(001)

We first present in this section our results for the coupling in Co/Cu(001) obtained numerically from Eqs. (16) and (17). The Green's functions $g_{\nearrow}^{\sigma}$ and g_r^{σ} have been calculated by the method of adlayers [see Eq. (6)] using the same set of tight-binding parameters as in Sec. II. Special care has been taken to ensure convergence of the sum over $\vec{k}_{\parallel}$ and of the energy integral. The latter was carried out in the complex energy plane and replaced by a sum over Matsubara frequencies. For temperatures close to room temperature, we found that the energy summation converges if one includes 10–15 Matsubara frequencies. All the results shown subsequently were obtained using 15 Matsubara frequencies. The summation over $\vec{k}_{\parallel}$ was performed using a dense mesh in the two-dimensional Brillouin zone. The numerical calculations reported here have all been performed for $T=316$ K.

We first discuss the results for the interlayer coupling between semi-infinite Co layers. They are shown in Fig. 10 for different numbers of points in the $\vec{k}_{\parallel}$ sum (231, 435, 2775). It is clear that convergence for large Cu thickness N can be achieved only with a very large number of points (2775) in the irreducible two-dimensional Brillouin zone. The numerical results clearly indicate that the short-period contribution coming from the Cu FS neck is dominant, in agreement with the quantum-well calculation of Sec. II. To further clarify this point, we apply the stationary-phase method to our cleavage formula for the coupling, which allows us again to separate analytically the contributions from the belly and necks of the Cu FS.

Similarly to the normalized spectral density, the integrand

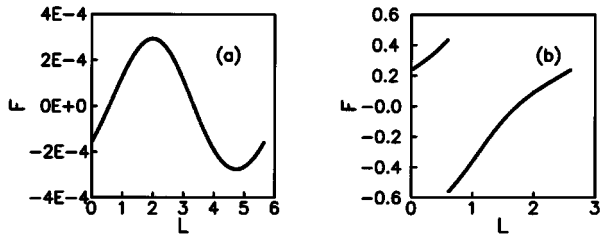

FIG. 11. (a) Integrand $F(\vec{k}_\parallel,E,N)$ of Eq. (16), at the Fermi energy and for $\vec{k}_\parallel=0$ (belly) shifted to the first period $(0,\pi/k_\perp)$; (b) same for the neck.

$F(\vec{k}_\parallel,E,N)$ in Eq. (17) is a periodic function of N and can be expanded in a Fourier series with the same wave vector $k_\perp(E,\vec{k}_\parallel)$. The corresponding Fourier coefficients $c_s(E,\vec{k}_\parallel)$ can be calculated by shifting the points for discrete spacer thicknesses, as described in Sec. II. The shifted points fall on a sectionally continuous function defined in the interval $(0,\pi/k_\perp)$, and can be immediately Fourier analyzed. Figures 11(a) and 11(b) show the shifted curves for the belly and the neck, respectively. The discontinuity that appears in the curve for the neck arises because of the formation of a bound state due to full confinement in the minority-spin channel. Such a bound state leads to a jump of π in the imaginary part of the logarithm in Eq. (17). Once the Fourier coefficients are determined, both integrations over $\vec{k}_\parallel$ and energy can be carried out analytically, following the same steps described in Sec. II. The expression for the coupling per surface atom then reads

$$J=\mathrm{Im}\sum_{k_\parallel^0}\sum_{s=1}^{\infty}\frac{\tau|c_s|e^{2i(sNk_\perp d+\psi_s)}}{2sNd}\times\frac{k_BT\left|\frac{\partial^2k_\perp}{\partial k_x^2}\frac{\partial^2k_\perp}{\partial k_y^2}\right|^{-1/2}}{\sinh\left[2\pi k_BT\left(sNd\frac{\partial k_\perp}{\partial E}+\frac{\partial\psi_s}{\partial E}\right)\right]},\qquad(22)$$

where $2\psi_s$ is the phase of the Fourier coefficient c_s. The sum over $\vec{k}_\parallel^0$ covers all the stationary points of $k_\perp$. It should be noted that Eqs. (22) and (5) are not identical because the functions that are Fourier analyzed are different. This is reflected in the Fourier coefficients and, hence, in the structure of Eqs. (22) and (5).

We compare in Fig. 12 our numerical results based on Eqs. (16) and (17) (dashed line) with the SPA calculation (solid line) based on Eq. (22), for $T=316$ K. The dashed line in Fig. 12 was obtained by Umerski's method for continuous N discussed in Sec. III; squares indicate the positions of atomic planes, i.e., the physical Cu thickness. The agreement between the two calculations is impressive and entirely justifies the stationary-phase approach. Comparing the continuous curve in Fig. 12 for the SPA based on the cleavage formula (17) with that of Fig. 9, which is based on the spectral density in the Cu spacer [Eq. (5)], we find only a small difference in amplitude and phase. It is clear from the results

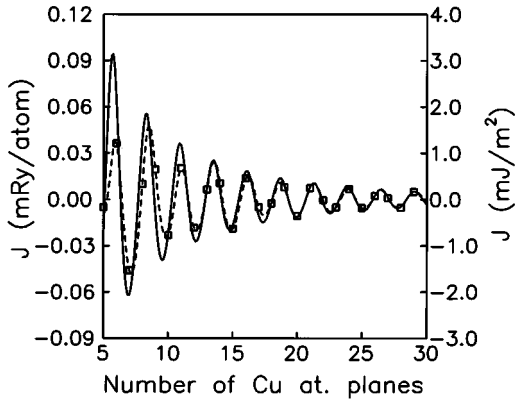

FIG. 12. Comparison between the numerical results (squares) and the stationary-phase calculation (full line) based on Eq. (22) for $T=316$ K. The dashed line is the result of a calculation using the closed-form solution to the Green's functions.

that the SPA formula based on the spectral density in the spacer leads to a slight underestimate of the coupling strength.

Given the high accuracy of the SPA calculation, we have used Eq. (22) to calculate the coupling for large Cu thicknesses (up to 100 atomic planes) both at zero and room temperatures to assess the approach of the coupling to the usual asymptotic form $\propto 1/N^2$. The results are shown in Fig. 13. It is clear that Cu thicknesses as large as 50 atomic planes are needed to reach the conventional asymptotic regime at zero temperature, and it is never reached at room temperature relevant to experiment. This shows that fits to the results of numerical calculations or to the experimental values of the coupling in Co/Cu(001) based on the conventional asymptotic dependence $1/N^2$ are unreliable.

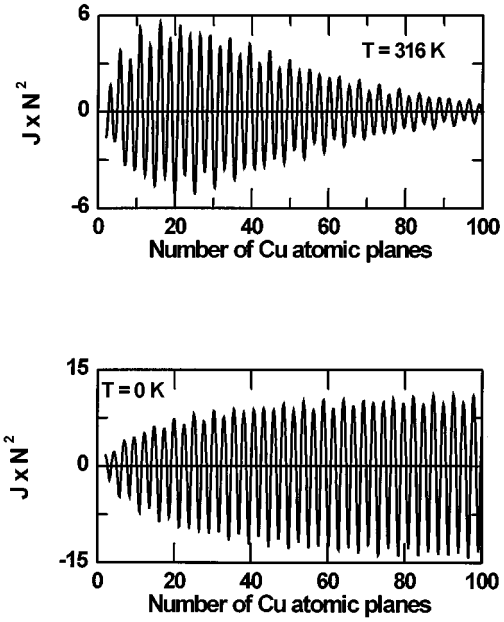

FIG. 13. Dependences of $J\times N^2$ on the number N of atomic planes of Cu obtained from the stationary-phase formula (22) at room and zero temperatures (J is measured in mRy per surface atom).

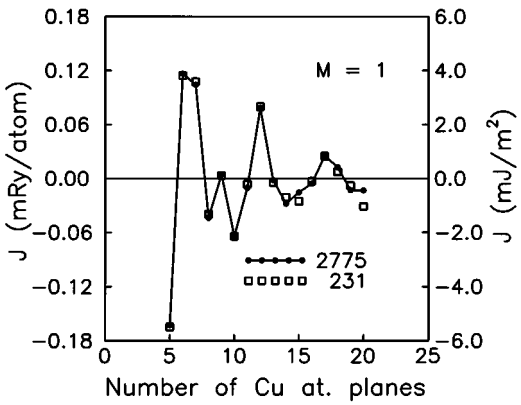

FIG. 14. Exchange coupling between two Co monolayers embedded in Cu for two different numbers of $\vec{k}_{\parallel}$ points in the irreducible Brillouin zone: $N_{\parallel}=231$ (squares), $N_{\parallel}=2775$ (full circles).

Finally, we return to the discussion of the relative weights of the contributions from the neck and belly extrema of the Cu FS. This is an interesting and fundamentally important problem since a simple Ruderman-Kittel-Kasuya-Yosida (RKKY) -type theory[35] predicts that the relative weights of these two contributions to the coupling are determined entirely by the curvatures of the Cu FS at the extremal points. Based on this argument, the RKKY theory predicts[35] comparable amplitudes of the belly and neck contributions to the coupling. Rather interestingly, the early calculations of Lang *et al.*[20] for Co monolayers embedded in Cu also show that long- and short-period oscillations have comparable amplitudes.

Our SPA calculation of the coupling for semi-infinite Co layers, described in Sec. II and in this section (see also Ref. 13), is in sharp contrast with all these results. It shows that the belly (long-period) contribution to the coupling is negligible. This is clear from a comparison of the belly contribution shown in Fig. 5 with the neck contribution to the coupling shown in Fig. 9. The same conclusion was reached independently by Kudrnovsky and co-workers[22,19] on the basis of a Fourier analysis of the coupling for semi-infinite Co layers. This is also confirmed by the calculations of Nordström *et al.*[21] and Lang *et al.*[36] for Co layers up to 11 ML thick that show that the neck (short-period) contribution becomes dominant. The advantage of the SPA method is that it allows rigorous separation of the coupling into its different oscillatory components, yielding their amplitudes, periods, and phases at any temperature.

Given the discrepancy between our results for semi-infinite Co layers and the early results of Lang *et al.*[20] for Co monolayers, we have also determined the coupling for two Co monolayers embedded in Cu. We have used in this fully numerical calculation based on Eq. (17) the same set of tight-binding parameters as in our calculation for the trilayer with semi-infinite Co. The results obtained with 231 and 2775 $\vec{k}_{\parallel}$ points in the irreducible two-dimensional Brillouin zone are shown in Fig. 14. It is clear from Fig. 14 that convergence in this case is achieved with a relatively small number (231) of $\vec{k}_{\parallel}$. We recall that at least 2775 points are necessary for infinitely thick Co layers. It can also be seen that the initial coupling strength is much larger (0.1 mRy/atom $\sim$3.4 mJ/m^2) than for semi-infinite Co. Our results for Co monolayers are in excellent agreement with those reported by Lang *et al.*[20] On the other hand, the amplitude of the dominant short-period oscillation obtained by Nordström *et al.*[21] and Lang *et al.*[36] for thicker Co layers (five atomic planes) remains a factor of almost 3 larger than our results for semi-infinite Co. This is almost certainly due to the fact that five atomic planes of Co is not enough to reach the asymptotic regime of thick (semi-infinite) Co layers considered in our calculations. It is worth noting that our results for semi-infinite Co layers are in excellent agreement with the LMTO calculations of Ref. 19 for the same system. It is interesting that such a very good agreement (the discrepancy between the two calculations is smaller than 5%) is obtained when we use the Cu hopping parameters at the Co/Cu interface. When the geometric mean of the Co and Cu hopping parameters is used instead, the overall coupling amplitude increases by about 35%.

V. CONCLUSIONS

We have described two complementary approaches for calculating the exchange coupling in magnetic multilayers. The first one is based on an asymptotic expansion of the thermodynamic potential valid for relatively large spacer thicknesses (SPA). This method provides a clear physical picture of the coupling, relating the oscillation periods to extremal dimensions of the spacer FS, and the coupling strength and phase to the degree of confinement of carriers in the spacer layer. The latter is determined by matching of the bulk ferromagnet and spacer bands in the direction perpendicular to the layers at the extremal points of the spacer FS. In addition, the SPA permits an analytic separation of the contributions to the coupling from each extremal point of the spacer FS. It also allows us to separate the contributions of up- and down-spin electrons in the ferromagnetic and antiferromagnetic configurations of the trilayer. Finally, because the coupling is linked in this approach directly to the spacer spectral density, it demonstrates explicitly that oscillations of the photoemission intensity[10–12] and oscillations of the exchange coupling have the same origin, i.e., the passage of quantum-well states across the FS as the thickness of the spacer is varied. The only limitation of this approach as presented here is that the spacer Fermi surface can only have a single sheet for each $\vec{k}_{\parallel}$. This is of course satisfied for Co/Cu(001). The generalization of the SPA asymptotic formula to a multisheet FS was described in Refs. 14 and 23 for a single-orbital tight-binding band. The application of the SPA method to the most general case of multiorbital band structure and multisheet FS will be described elsewhere.

The second approach is fully numerical and has no such restriction. It is based on a new cleavage formula for the coupling that has an exact correspondence with our original quantum-well theory of the coupling.[5,6] Moreover, the derivation of the cleavage formula presented in Sec. III shows explicitly that, for a single-orbital tight-binding band, the cleavage formula is equivalent to the torque (spin-current) formula for the coupling.[25]

The cleavage formula is very convenient from the computational point of view since local one-electron Green's functions in only two neighboring atomic planes of the spacer are required to calculate the coupling. It follows that

the calculation of the coupling for magnetic layers of arbitrary thicknesses requires no more computational effort than the calculation for magnetic layers containing just one atomic plane. The stationary phase method can also be applied to the cleavage formula, which leads to an alternative asymptotic expression for the coupling.

Finally, using the method of Umerski,[15] which yields closed-form expressions for the local Green's functions in any layer structure, the coupling can be computed entirely numerically from the cleavage formula for fractional values of the interplanar distance d. This method provides a dense set of points for the coupling restricted to a relatively thin spacer that can be reliably analyzed numerically for periods, amplitudes, and phases of all the oscillatory contributions to the coupling. To achieve the same degree of accuracy with the conventional numerical methods, which give the coupling on discrete atomic planes only, one would have to go to very large spacer thicknesses where the convergence in the $\vec{k}_{\parallel}$ space becomes poor.

As an illustration, we investigated comprehensively the oscillatory exchange coupling in Co/Cu(001) using the two approaches described above. In both calculations, the same tight-binding parametrization of an *ab initio* band structure of Cu and Co was used. The results of the fully numerical calculation for a Co/Cu(001) trilayer with semi-infinite Co, based on our new cleavage formula for the coupling, are in excellent agreement with the results obtained from the asymptotic expansion of the spectral density (the original quantum-well theory with SPA), as well as with the results of the SPA applied to the cleavage formula. The use of the stationary-phase approximation for systems such as Co/Cu is, therefore, fully justified and brings all the advantages listed above. In particular, the numerical calculation confirms the result of the SPA that the short-period (neck) oscillation dominates the coupling in Co/Cu(001) with thick Co layers, the long-period (belly) oscillation being negligible. The SPA approach allows us to interpret this result as being due to complete confinement in the FM configuration of the minority electrons at the Cu FS necks. The quantum-well states at the Cu FS neck were recently observed by photoemission.[12]

The SPA asymptotic formula also shows that the initial decay of the coupling with Cu thickness is much slower than the $1/N^2$ law that usually holds at $T=0$ K. In fact, the regime in which the $1/N^2$ law holds is reached only for $N \approx 50$ at zero temperature and is never reached at room temperature. This occurs because of the strong energy dependence of the phase of the coupling, which is due to complete confinement of the minority carriers at the Cu FS necks. On the other hand, the asymptotic decay of the belly contribution to the coupling obeys the usual $1/N^2$ law. We stress that the SPA method provides for each component of the oscillatory coupling the correct dependence [Eq. (22)] on the Cu thickness N at an arbitrary temperature. The dependences on Cu thickness obtained from Eq. (22) are very accurate beginning from some 10 atomic planes of Cu and these are the asymptotic laws that should be used to analyze experimental data and the results of numerical calculations.

The strong energy dependence of the phase at the Cu FS necks leads also to a strong temperature dependence of the total coupling which is dominated by the neck contribution. The belly contribution, on the other hand, hardly changes at all between zero and room temperatures.

There is now a theoretical consensus (Refs. 22,13,21, and 37) that the short-period (neck) contribution to the coupling in Co/Cu(001) with thick Co layers dominates the total coupling. However, the magnitude of the coupling at the first antiferromagnetic peak ≈ 1.2 mJ/m^2 we have determined numerically from the cleavage formula is a factor of almost 3 smaller than the result of Nordström *et al.* and Lang *et al.* for Co layers containing five atomic planes of Co.[21,36] This is most likely due to the fact that the asymptotic limit of thick (semi-infinite) Co layers we consider was not reached in their calculations. Rather interestingly, the coupling we obtain for 2 ML of Co embedded in Cu is virtually identical to the coupling curve obtained by Lang *et al.*[20] for the same system. There is, therefore, complete agreement between the two sets of calculations for Co monolayers. They show a much larger total coupling strength ≈ 3.4 mJ/m^2 and comparable amplitudes of the short- and long-period oscillations.

Finally, we comment on the SPA calculation of Lee and Chang,[37] which is based on the reflection coefficient method of Bruno and Stiles.[8,9] The coupling strength reported by Lee and Chang is a factor of 8 larger than the value ≈ 1.2 mJ/m^2 we obtain. This is almost certainly due to the fact that they have neglected in the SPA the energy dependence of the phase, which is a crucial factor at the neck extrema of the Cu FS.

As far as the experimental situation is concerned, the experimental results of Johnson *et al.*[34] for thick Co layers seem to indicate that the amplitudes of the short- and long-period oscillations of the coupling are comparable. This contradicts all the theoretical results referred to above, but it has to be borne in mind that all the calculations were made assuming perfect Co/Cu interfaces. It is reasonable to expect that interfacial roughness would tend to suppress the short-period oscillations. In fact, most recent experiments of Weber, Allenspach, and Bischof[38] using a scanning electron miscroscope with polarization analysis (SEMPA), which were performed on a series of Co/Cu samples, show that, while the long-period oscillation is seen in samples with relatively ''poor'' interfaces, the short-period oscillation becomes totally dominant for the ''best'' samples. Weber, Allenspach, and Bischof[38] estimate that, for their best samples, the amplitude of the short-period oscillation is a factor of 7 larger than that of the long-period oscillation. Unfortunately, SEMPA does not yield the absolute values of the coupling. It would, therefore, be very desirable to perform MOKE measurements on the best samples of Weber, Allenspach, and Bischof. Such measurements might well yield a greater coupling strength, i.e., closer to the calculated values than the coupling strength obtained by Johnson *et al.*[34]

ACKNOWLEDGMENTS

The support of the Engineering and Physical Sciences Research Council (EPSRC UK), CNPq of Brazil, and North Atlantic Treaty Organization (NATO Grant No. CRG 950800) is gratefully acknowledged. One of us (M.V.) would also like to thank the Nuffield Foundation (U.K.) for financial support.

[1] S. S. P. Parkin, N. More, and K. P. Roche, Phys. Rev. Lett. **64**, 2304 (1990).
[2] M. N. Baibich, J. M. Broto, A. Fert, F. Van Dau Nguyen, F. Petroff, P. Etienne, G. Creuzet, A. Friederich, and J. Chazelas, Phys. Rev. Lett. **61**, 2472 (1988).
[3] *Ultrathin Magnetic Structures 1: An Introduction to the Electronic, Magnetic and Structural Properties*, edited by J. A. C. Bland and B. Heinrich (Springer, Berlin, 1994).
[4] D. M. Edwards and J. Mathon, J. Magn. Magn. Mater. **93**, 85 (1991).
[5] D. M. Edwards, J. Mathon, R. B. Muniz, and M. S. Phan, Phys. Rev. Lett. **67**, 493 (1991); J. Phys.: Condens. Matter **3**, 4941 (1991).
[6] J. Mathon, M. Villeret, and D. M. Edwards, J. Phys.: Condens. Matter **4**, 9873 (1992).
[7] J. Mathon, M. Villeret, and D. M. Edwards, J. Magn. Magn. Mater. **127**, L261 (1993).
[8] P. Bruno, Phys. Rev. B **52**, 411 (1995).
[9] M. D. Stiles, Phys. Rev. B **48**, 7238 (1993).
[10] J. E. Ortega and F. J. Himpsel, Phys. Rev. Lett. **69**, 844 (1992).
[11] J. E. Ortega, F. J. Himpsel, G. J. Mankey, and R. F. Willis, Phys. Rev. B **47**, 1540 (1993).
[12] P. Segovia, E. G. Michel, and J. E. Ortega, Phys. Rev. Lett. **77**, 3455 (1996).
[13] J. Mathon, M. Villeret, R. B. Muniz, J. d'Albuquerque e Castro, and D. M. Edwards, Phys. Rev. Lett. **74**, 3696 (1995).
[14] J. d'Albuquerque e Castro, J. Mathon, M. Villeret, and D. M. Edwards, Phys. Rev. B **51**, 12 876 (1995).
[15] A. Umerski, Phys. Rev. B **55**, 5266 (1997).
[16] F. Herman, J. Sticht, and M. van Schilfgaarde, J. Appl. Phys. **69**, 4783 (1991); in *Magnetic Surfaces, Thin Films, and Multilayers*, edited by S. S. P. Parkin, H. Hopster, J.-P. Renard, T. Shinjo, and W. Zinn, MRS Symposia Proceedings No. 231 (Materials Research Society, Pittsburgh, 1992), p. 195; in *Physics of Transition Metals 1*, edited by P. M. Oppeneer and J. Kuebler (World Scientific, Singapore, 1993).
[17] S. Krompiewski, F. Suss, and U. Krey, Europhys. Lett. **26**, 303 (1994).
[18] M. van Schilfgaarde and F. Herman, Phys. Rev. Lett. **71**, 1923 (1993); M. van Schilfgaarde, F. Herman, S. S. P. Parklin, and J. Kudrnovsky, *ibid.* **74**, 4063 (1995).
[19] V. Drchal, J. Kudrnovsky, I. Turek, and P. Weinberger, Phys. Rev. B **53**, 15 036 (1996).
[20] P. Lang, L. Nordström, R. Zeller, and P. H. Dederichs, Phys. Rev. Lett. **71**, 1927 (1993).
[21] L. Nordström, P. Lang, R. Zeller, and P. H. Dederichs, Phys. Rev. B **50**, 13 058 (1994).
[22] J. Kudrnovsky, V. Drchal, I. Turek, and P. Weinberger, Phys. Rev. B **50**, 16 105 (1994).
[23] M. Fereira, J. d'Albuquerque e Castro, D. M. Edwards, and J. Mathon, J. Phys.: Condens. Matter **8**, 11259 (1996).
[24] J. Kudrnovsky, V. Drchal, I. Turek, M. Sob, and P. Weinberger, Phys. Rev. B **53**, 5125 (1996).
[25] D. M. Edwards, A. M. Robinson, and J. Mathon, J. Magn. Magn. Mater. **140-144**, 517 (1995).
[26] J. C. Slonczewski, Phys. Rev. B **39**, 6995 (1989).
[27] J. d'Albuquerque e Castro, M. S. Ferreira, and R. B. Muniz, Phys. Rev. B **49**, R16 062 (1994).
[28] J. d'Albuquerque e Castro, J. Mathon, M. Villeret, and A. Umerski, Phys. Rev. B **53**, R13 306 (1996).
[29] D. A. Papaconstantopoulos, *Handbook of The Band Structure of Elemental Solids* (Plenum, New York, 1986).
[30] V. L. Moruzzi, J. F. Janak, and A. R. Williams, *Calculated Electronic Properties of Metals* (Pergamon, Oxford, 1978).
[31] D. H. Lee and J. D. Joannopoulos, Phys. Rev. B **23**, 4988 (1981).
[32] J. Mathon, J. Phys.: Condens. Matter **1**, 2505 (1989).
[33] M. P. Lopez Sancho, J. M. Lopez Sancho, and J. Rubio, J. Phys. F **15**, 851 (1985).
[34] M. T. Johnson, P. J. H. Bloemen, R. Coehoorn, J. J. de Vries, N. W. E. McGee, R. Jumgblut, A. Reinders, and J. aan de Stegge, in *Magnetic Ultrathin Films, Multilayers, and Surfaces/ Interfaces and Characterization*, edited by B. T. Jonker, S. A. Chambers, R. F. C. Farrow, C. Chappert, R. Clarke, W. J. M. de Jonge, T. Egami, P. Grünberg, K. M. Krishnan, E. E. Marinero, C. Rau, and S. Tsunashima, MRS Symposia Proceedings No. 313 (Materials Research Society, Pittsburgh, 1993), p. 93.
[35] P. Bruno and C. Chappert, Phys. Rev. Lett. **67**, 1602 (1991); Phys. Rev. B **46**, 261 (1992).
[36] P. Lang, L. Nordström, K. Wildberger, R. Zeller, and P. H. Dederichs, and T. Hoshino, Phys. Rev. B **53**, 9092 (1996).
[37] B. Lee and Y.-Ch. Chang, Phys. Rev. B **52**, 3499 (1995).
[38] W. Weber, R. Allenspach, and A. Bischof, Europhys. Lett. **31**, 431 (1995).